Ding *et al. Journal of Ovarian Research* (2024) 17:250
https://doi.org/10.1186/s13048-024-01573-3

Journal of Ovarian Research

RESEARCH Open Access

Bile acids in follicular fluid: potential new therapeutic targets and predictive markers for women with diminished ovarian reserve

Shu Ding[1†], Wenyan Li[2†], Xianglei Xiong[1], Manfei Si[1,3,4,5], Chuyu Yun[1,3], Yuqian Wang[1,4,5], Lixuan Huang[1,3,4,5], Sen Yan[1,3,4,5], Xiumei Zhen[1,3,4,5], Jie Qiao[1,3,4,5] and Xinyu Qi[1,3,4,5,6*]

Abstract

Objective To investigate the changes in bile acid (BA) metabolites within the follicular fluid (FF) of patients with diminished ovarian reserve (DOR) and to identify novel diagnostic markers that could facilitate early detection and intervention in DOR patients.

Design A total of 182 patients undergoing assisted reproductive technology (ART) were enrolled and categorized into the normal ovarian reserve (NOR) group ($n=91$) or the DOR group ($n=91$) to measure BA levels in FF. To identify the changes in granulosa cells (GCs), we collected GCs from an additional 7 groups of patients for transcriptome sequencing.

Setting Reproductive medicine center within a hospital and university research laboratory.

Population A total of 182 patients undergoing assisted reproductive technology were enrolled and categorized into the NOR group ($n=91$) or the DOR group ($n=91$).

Methods In this study, BA metabolites in FF of DOR and NOR patients were analyzed in detail by targeted metabolomics, and the correlation between BA levels in FF and clinical indicators was discussed. Then, we constructed a diagnostic model for DOR using the random forest algorithm based on five different BAs. Additionally, we performed a functional enrichment analysis on differentially expressed genes (DEGs) in GCs from both DOR and NOR patients.

Main outcome measures BA levels in FF and their correlation with clinical indicators; the areas under the curve (AUCs) of the random forest diagnostic model for DOR; and the DEGs and corresponding functional enrichment results of GC RNA analysis.

Result (s) The levels of lithocholic acid, chenodeoxycholic acid, ursodeoxycholic acid, deoxycholic acid and cholic acid in FF of DOR group were lower than those of NOR group. And significant reductions in total, primary, secondary, and unconjugated BA levels were observed in the DOR group. The above five BAs levels were closely related to

[†]Shu Ding and Wenyan Li contributed equally to this work.

*Correspondence:
Xinyu Qi
qixinyu@bjmu.edu.cn

Full list of author information is available at the end of the article

indicators of ovarian reserve. The AUC of the diagnostic model based on the above five BAs was 0.964. Based on transcriptome sequencing data from two groups of GCs, a total of 482 up-regulated and 654 down-regulated DEGs were identified. Gene ontology analysis revealed that the metabolic and biosynthetic processes of fatty acids, steroids, and cholesterol were enriched in these DEGs, whereas Kyoto Encyclopedia of Genes and Genomes analysis indicated enrichment of fatty acid and ovarian steroidogenesis.

Conclusion(s) The levels of multiple BA metabolites in FF are significantly lower than those in patients with DOR and are closely related to the evaluation of ovarian reserve function.

Introduction

The ovary, as the pivotal reproductive organ in women, is responsible for egg production and ovulation, as well as the synthesis and secretion of estrogen, progesterone (P), and a small amount of androgen. The close relationship between the ovary and female fertility is well established [13]. However, ovarian aging and disease-induced declines in ovarian response leads to reduced endocrine function and a subsequent decrease in oocyte quantity and quality, which significantly impacts reproductive function [47]. Diminished ovarian reserve (DOR) is characterized by a reduction in the number and/or quality of oocytes, accompanied by decreased anti-Mullerian hormone (AMH) levels, reduced antral follicle count (AFC), and increased follicle-stimulating hormone (FSH) levels. Clinical manifestations of DOR include oligomenorrhea, hypomenorrhea, infertility, or infertility before the age of 40, and DOR can progress to premature ovarian insufficiency (POI) or premature ovarian failure (POF) [4, 16, 18, 37, 42, 43]. But the currently recognized indicators for assessing ovarian reserve cannot detect DOR early enough to initiate interventions in time. Ovarian aging is a pathophysiological process involving multiple factors and mechanisms. Genetic variation, oxidative stress, mitochondrial dysfunction, chronic inflammation and fibrosis can affect ovarian reserve and ovarian microenvironment, leading to DOR. However, the underlying cause is unknown [37]. As the complex and unclear etiology of DOR, coupled with its insidious onset and multifactorial pathogenesis, poses a significant challenge for infertility treatment and prevention.

The ovarian microenvironment, particularly the local follicular environment, is crucial for egg development. The primary components of this microenvironment are cumulus cells and follicular fluid (FF). FF, which is derived from plasma components and follicular cell secretions, contains numerous proteins, cytokines, growth factors, peptide hormones, steroids, energy metabolites, and other unknown components, all of which are vital for follicle development. The composition of FF mirrors the microenvironment that encompasses the oocyte and is closely linked to both follicular development and the competence of the oocyte. It holds potential as a valuable medium for investigating the underlying mechanisms of various ovarian diseases [12]. A number of studies have described how ovarian function is affected by metabolite changes in the FF of women with DOR, with particular impacts of metabolites in choline metabolism [46], tryptophan metabolism [29], aminoacyl tRNA biosynthesis [29], purine metabolism [29], indole metabolism [33], arginine metabolism [11], oxidative stress and inflammatory processes [22]. However, studies on the relationship between the metabolites of the bile acids (BAs) and DOR are still poorly understood.

BAs, steroids synthesized by the liver, are integral to bile synthesis and are related to glucose and lipid metabolism. It has been reported that the concentration of BAs in FF is twice that in serum, and the large amounts of BAs indicates that these compounds have an important effect on follicle development [41]. Recent research has highlighted the significant impact of BA metabolism on ovarian function [28; 48, 52, 59] 9]. Qi et al. demonstrated that glycodeoxycholic acid and tauroursodeoxycholic acid levels are decreased in polycystic ovary syndrome (PCOS) patients, suggesting that BA supplementation and metabolic improvement could be novel treatment strategies for PCOS [44]. It is necessary to be clear that PCOS is also a syndrome of decreased ovarian function due to abnormal sex hormone secretion, accompanied by metabolic disorders, which can lead to decreased fertility. Li et al. reported that the decrease of oocyte quality in mice under continuous light was related to embryonic development and the changes of intestinal microflora and their metabolites, then showed that secondary bile acids could effectively rescue the decrease of oocyte quality and embryonic development [29]. Additionally, increased concentrations of various secondary BAs in the intestine can lead to significant increases in the abundance of pro-inflammatory bacteria, thereby exacerbating oxidative stress and inflammatory responses in the intestine and potentially worsening ovarian function [30]. However, the role and impact of BA metabolites in the ovarian microenvironment of DOR patients remain incompletely understood.

Therefore, this study aimed to investigate the changes of BA metabolism in the FF of patients with DOR by targeted metabolomics, and attempted to explore the direct effects of BA changes on ovarian function by studying the transcriptome changes of granulosa cells (GCs) in patients with DOR. We hope to identify metabolic

factors influencing oocyte quality and to discover novel diagnostic markers, which may offer valuable insights for the early detection and intervention of patients with DOR.

Materials and methods

Patients

We recruited 182 patients under 40 years old from February 2023 to April 2023, who were undergoing assisted reproductive technology (ART) treatment in the Centre for Reproductive Medicine, Peking University Third Hospital. Of the 182 women, 91 were assigned to the DOR group, and 91 were assigned to the normal ovarian reserve (NOR) group. This study was approved by the Ethics Committee of Medical Scientific Research at Peking University Third Hospital, and informed consent was obtained from all participants (Peking University Third Hospital Ethics Committee No. M2023152).

Women were diagnosed with DOR based on at least two of the following established criteria [56]: (a) AMH < 1.1 ng/mL; (b) AFC < 7 follicles; and (c) FSH > 10 mIU/mL. The NOR group consisted of women with regular menstrual cycles, normal ovarian morphology, and normal hormone levels who were seeking ART due to male factor infertility or tubal factors. The exclusion criteria included chromosomal abnormalities, ovarian surgery, PCOS, polycystic ovaries, endometriosis, recurrent spontaneous abortion, intestinal or liver diseases, and metabolism-related diseases.

Assessment of clinical pregnancy outcomes

Patients received individualized stimulation protocols recommended by the hospital according to their own conditions, and oocytes were retrieved 36 h after human chorionic gonadotrophin (hCG) administration. Choose different fertilization methods according to the plan given by an experienced doctor. Each oocyte retrieved was inseminated with 10,000 motile spermatozoa during in vitro fertilization (IVF) cycles. Mature (metaphase II [MII]) oocytes were identified by the presence of a first polar body (PB) and subsequently used for intracytoplasmic sperm injection (ICSI). Normal fertilization was confirmed by the presence of two pronuclei (PN) and a second PB 16–18 h post insemination. The normal fertilization rate was calculated by dividing the number of 2PN fertilized oocytes by the total number of oocytes in IVF or dividing the number of 2PN fertilized oocytes by the number of MII oocytes in ICSI. At 67–69 h post insemination (Day 3), embryo quality was assessed based on cell number and the degree of cytoplasmic fragmentation. The transplantable embryo rate was determined by dividing the number of embryos that developed from 2PN to the five- or more-cell stage with less than 30% fragmentation on Day 3 by the number of cleaved embryos on Day 2. Ultimately, embryos on Day 3, Day 5, or Day 6 were transferred according to each patient's condition [38].

Clinical outcomes of the fresh cycle were defined as follows: biochemical pregnancy: serum β-hCG level > 10 IU/L measured 14 days after embryo transfer; clinical pregnancy: visualization of at least one gestational sac by ultrasound 30 days after embryo transfer; live birth: the birth of one or more live infants; and pregnancy loss: ectopic pregnancy or abortion before 28 weeks of gestation .

Data collection

We collected data on maternal age, body mass index (BMI), infertility diagnosis (primary or secondary infertility), duration of infertility (years), male factor infertility, baseline serum sex hormones, AMH and AFC. Serum sex hormones and AMH were detected in all patients by radio-immunoassay and bilateral AFCs on menstrual cycle day 2–3 was calculated by transvaginal ultrasonography. During IVF or ICSI, the following factors were included in the analysis: type of fertilization, days of stimulation, gonadotropins dose, serum sex hormones levels on the day of hCG injection, endometrial thickness, the number of oocytes retrieved, normal fertilization rate, cleavage rate, available embryo rate, high quality embryo rate, number of embryos transferred, type of embryo transferred (cleavage embryo or blastocyst). Pregnancy outcome indicators included biochemical pregnancy, clinical pregnancy, live birth (singleton or multiple live births) and pregnancy loss (abortion or ectopic pregnancy).

All data on general patient characteristics and clinical pregnancy outcomes were obtained from electronic medical records, which were recorded and regularly quality controlled by a dedicated team.

Collection of follicular fluid and granulosa cells

During the retrieving of the oocytes, FF was collected in a sterile centrifuge tube. The FF was then centrifuged at 1500×g for 10 min to remove insoluble particles and cells. Then, 500 μL of the supernatant of FF was collected and stored at -80 °C for future analysis.

FF was drawn into a centrifuge tube, and after centrifugation, the upper white layer was carefully extracted, precipitated, and mixed with phosphate-buffered saline (PBS). Following centrifugation, the supernatant was discarded, and the cells in the upper layer were digested. After Ficoll separation, the white villous GCs were collected, washed twice with PBS, resuspended in DMEM-F12 medium supplemented with 10% bovine serum, and cultured for 8–12 h. The medium was then changed to remove nonadherent cells and blood cells; the adherent cells were GCs. 1 mL of TRI reagent was added to

the GCs, followed by cell lysis through pipetting up and down. The samples were stored at -80 °C before processing.

Targeted metabolomic analysis and determination of the total bile acid concentration

FF samples were slowly thawed at 4 °C prior to LC−MS/MS analysis. A 100 μL aliquot of FF from each group was mixed with 500 μL of methanol containing an internal standard (10 μL). BA standard solutions were mixed and diluted with methanol to achieve 12 different concentrations (500, 250, 100, 50, 25, 10, 5, 2.5, 1, 0.5, 0.25, and 0.1 ng/mL), with the internal standard added in proportion to the FF sample to establish the calibration curve. After shaking and centrifugation (14000×g, 4 °C, 20 min), the supernatant was transferred to a new centrifuge tube and freeze-dried. The residue was reconstituted with 100 μL methanol/water (1:1, v/v) and centrifuged at 14,000×g at 4 °C for 15 min, and the resulting supernatant was collected for LC−MS/MS analysis.

Development of the random forest model

The diagnostic model was developed using the R package randomForest (version 4.7–1.1). Ntree = 800 and mtry = 3 was set as the arguments for the random forest. All samples were randomly divided into two sets, with 70% (127 samples) used as the training set for training model. The remaining 30% (55 samples) was used as the validation set to evaluate the performance of the predictor. The R package pROC (version 1.18.5) was used to generate receiver operating characteristic (ROC) curves and to calculate the 95% confidence intervals (CIs) of the areas under the curve (AUCs). The mean decrease accuracy and mean decrease in the Gini coefficient were calculated to determine the variable importance in the random forest model, with higher values indicating greater importance.

RNA extraction and Illumina sequencing

The samples were thawed on ice and added 0.2 mL chloroform. The sample tube was securely capped and shaken vigorously for 15–20 s by hand. After incubation at room temperature for 5–10 min, the sample tube was centrifuged at 12,000×g for 15 min at 4 °C. The upper clear aqueous phase was carefully transferred to a new microcentrifuge tube, and 100% isopropanol was added for initial homogenization of the aqueous phase. After incubation at room temperature for 10 min, the sample was centrifuged at 12,000×g at 4 °C for 15 min; then, the supernatant was completely removed. The pellet was washed with 1 mL of 75% ethanol used for the initial homogenization and vortexed to mix well. The sample was centrifuged at 12,000×g at 4 °C for 5 min; then, the supernatant was completely removed. The RNA pellet was allowed to air dry at room temperature for 5–10 min. The total RNA was dissolved in 30 uL of RNase-Free ddH20.

RNA degradation and purity were assessed using 1% agarose gels and a NanoPhotometer® spectrophotometer (IMPLEN, CA, USA), respectively. RNA integrity was assessed using the RNA Nano 6000 Assay Kit of the Bioanalyzer 2100 system (Agilent Technologies, CA, USA). A total amount of 1 ug RNA per sample was used as input material for the RNA sample preparations. Sequencing libraries were generated using NEBNext® UltraTM RNA Library Prep Kit for Illumina® (NEB, USA) following manufacturer's recommendations and index codes were added to attribute sequences to each sample. The clustering of the index-coded samples was performed on a cBot Cluster Generation System using TruSeq PE Cluster Kit v3-cBot-HS (Illumia) according to the manufacturer's instructions. After cluster generation, the library preparations were sequenced on an Illumina Novaseq platform and 150 bp paired-end reads were generated.

Quality control and RNA-seq data analysis

Firstly, clean data were obtained by removing reads containing adapter, reads containing ploy-N, and low-quality reads from raw data. At the same time, Q20, Q30 and GC content the clean data were calculated. Reference genome indexing and alignment of paired-end clean reads were performed with Hisat2 v2.0.5. Subsequently, the mapped reads of each sample were assembled by StringTie (v1.3.3b) and featureCounts v1.5.0-p3 was used to count the reads numbers mapped to each gene. Finally, FPKM of each gene was calculated based on the length of the gene and reads count mapped to this gene.

Differentially expressed genes (DEGs) were identified using the R package DEseq2 (version 1.40.2), with an adjusted P value < 0.05 and $|\log_2$ (fold change; FC)$| > 0.58$ as the criteria for significance. DEGs were categorized as up-regulated or down-regulated. Gene Ontology (GO) and Kyoto Encyclopedia of Genes and Genomes (KEGG) functional enrichment analyses were conducted to annotate the biological functions of the DEGs using the R package clusterProfiler (version 4.8.3). A P value < 0.05 and a Q value < 0.05 were considered to indicate statistical significance.

Statistical analysis

Statistical analysis was performed using SPSS Statistics (version 27.0, IBM Corp., Armonk, New York), GraphPad Prism 9.0 (San Diego, CA, USA) and R software (version 4.3.1, R core team). Descriptive statistics are presented as the mean and standard deviation (SD) for continuous data and as the number and percentage for categorical data. Mann−Whitney U tests were used to compare continuous data means, while chi−square tests or Fisher's

Table 1 General patient characteristics and clinical pregnancy outcomes after a fresh cycle in the NOR and DOR groups

Variable	NOR (n = 91)	DOR (n = 91)	*P* value
Age, years	33.76 ± 0.36	34.26 ± 0.38	0.229
Body mass index, kg/m^2	22.23 ± 0.35	22.30 ± 0.33	0.612
Infertility diagnosis			1.000
Primary infertility	60 (65.9)	60 (65.9)	
Secondary infertility	31 (34.1)	31 (34.1)	
Duration of infertility, years	3.25 ± 0.30	3.91 ± 0.32	0.057
Male factor infertility	70 (76.9)	71 (78.0)	0.859
Baseline FSH, mIU/mL	6.13 ± 0.20	10.05 ± 0.47	< 0.001*
Baseline AMH, ng/mL	3.38 ± 0.17	0.61 ± 0.03	< 0.001*
Antral follicle count	14.32 ± 0.61	3.98 ± 0.28	< 0.001*
Baseline LH, IU/L	3.62 ± 0.20	3.46 ± 0.17	0.592
Baseline E_2, pmol/L	107.30 ± 12.81	161.07 ± 27.05	0.018*
Baseline P, ng/mL	1.23 ± 0.08	2.95 ± 1.56	0.579
Fertilization method			0.006*
IVF	41 (45.0)	56 (61.5)	
ICSI	44 (48.4)	35 (38.5)	
IVF + ICSI	6 (6.6)	0 (0)	
Duration of stimulation, days	10.35 ± 0.17	10.23 ± 0.27	0.572
Gonadotropins dose, IU	2523.43 ± 85.56	2992.92 ± 148.68	0.034*
LH on hCG day, IU/L	38.89 ± 36.51	20.28 ± 17.05	0.012*
E_2 on hCG day, pmol/L	10986.32 ± 647.84	3739.22 ± 298.61	< 0.001*
P on hCG day, ng/mL	2.45 ± 0.12	2.18 ± 0.38	< 0.001*
Endometrial thickness, mm	10.39 ± 0.16	9.35 ± 0.23	0.004*
No. of oocytes retrieved	12.04 ± 0.58	3.79 ± 0.26	< 0.001*
Normal fertilization rate	0.67 ± 0.02	0.62 ± 0.04	0.928
Cleavage rate	0.98 ± 0.01	0.94 ± 0.02	0.420
Available embryo rate	0.38 ± 0.03	0.41 ± 0.04	0.890
High quality embryo rate	0.47 ± 0.03	0.46 ± 0.04	0.850
No. of embryos transferred			< 0.001*
1	2/47 (4.3)	20/45 (44.4)	
2	45/47 (95.7)	25/45 (55.6)	
Type of embryo transferred			0.144
Cleavage embryo	47/47 (100.0)	43/45 (95.6)	
Blastocyst	0/47 (0.0)	2/45 (4.4)	
Biochemical pregnancy	25/47 (53.2)	22/45 (48.9)	0.835
Clinical pregnancy	25/47 (53.2)	21/45 (46.7)	0.677
Pregnancy loss	3/25 (12.0)	4/21 (19.0)	0.686
Live birth			0.381
Singleton live birth	17/47 (36.2)	14/45 (31.1)	
Multiple live births	5/47 (10.6)	3/45 (6.7)	

Note Continuous data are reported as the mean ± standard deviation. Categorical data are reported as n (%). The Mann–Whitney U test was used to analyze continuous data, and the chi–square test or Fisher's exact test was used to analyze categorical data. NOR = normal ovarian reserve; DOR = diminished ovarian reserve. * $P < 0.05$

exact tests were used to compare categorical data percentages. The Spearman correlation coefficient was calculated using the R package psych (version 2.4.3). All *P* values were two-sided, with $P < 0.05$ considered to indicate statistical significance.

Results

General patient characteristics and clinical pregnancy outcomes

The demographic and assisted reproductive-related data for 182 patients are summarized in Table 1. No significant differences were found in age, BMI, infertility diagnosis, duration of infertility, or male factor infertility rate between the NOR and DOR groups. However, there were significant differences between groups in baseline FSH, AMH, and AFC levels, consistent with the clinical characteristics of DOR patients. Notably, baseline estradiol (E_2) levels were significantly higher in the DOR group.

There was a significant difference in assisted reproductive fertilization method between the two groups, primarily due to the choice of IVF+ICSI by patients in the NOR group. After excluding IVF+ICSI, the difference in fertilization method was no longer significant. During ART, there was no difference between groups in the number of stimulation days required, although the DOR group required a larger dose of gonadotropins. Luteinizing hormone (LH), E_2, and P levels on the day of hCG injection, endometrial thickness, and the number of oocytes retrieved were significantly higher in the NOR group than in the DOR group. No significant differences were found in the normal fertilization rate, cleavage rate, available embryo rate, high-quality embryo rate, type of embryo transferred, biochemical pregnancy rate, clinical pregnancy rate, abortion rate, or live birth rate. However, the rate of two-embryo transfer was significantly lower in the DOR group.

Differences in bile acid metabolite levels in follicular fluid

A total of 16 BA metabolites were identified in FF (Table 2). Compared to the NOR group, the DOR group showed reduced levels of five distinct BA metabolites: lithocholic acid (LCA), chenodeoxycholic acid (CDCA), ursodeoxycholic acid (UDCA), deoxycholic acid (DCA) and cholic acid (CA). The level of total BAs in FF was also significantly decreased in the DOR group (Fig. 1A). Further analysis of BA metabolites revealed that both primary and secondary BA levels were significantly decreased in the DOR group (Fig. 1B and C). Concurrently, unconjugated BA levels were reduced in the FF of DOR patients (Fig. 1D). However, the concentration of conjugated BAs was similar between the two groups (Fig. 1E).

Table 2 Expression profile of bile acid metabolites in FF from the NOR and DOR groups

Bile Acid Metabolites (nmol/L)	NOR ($n=91$)	DOR ($n=91$)	*P* value
LCA	86.89 ± 3.59	24.36 ± 1.32	< 0.001*
CDCA	361.58 ± 31.96	106.99 ± 10.86	< 0.001*
UDCA	141.15 ± 16.50	32.88 ± 4.71	< 0.001*
DCA	740.80 ± 69.16	351.24 ± 40.41	< 0.001*
CA	197.37 ± 24.54	111.44 ± 17.07	< 0.001*
GCDCA	782.61 ± 47.55	654.21 ± 36.65	0.099
GUDCA	357.90 ± 39.32	241.34 ± 27.76	0.100
TLCA	6.07 ± 0.71	4.96 ± 0.59	0.395
GCA	147.85 ± 12.44	173.16 ± 6.99	0.419
GDCA	585.96 ± 71.60	561.92 ± 48.95	0.419
GLCA	47.21 ± 6.26	43.36 ± 6.06	0.577
TCDCA	45.88 ± 3.14	45.81 ± 3.73	0.747
THDCA	2.75 ± 0.19	2.75 ± 0.22	0.747
TCA	18.17 ± 1.69	20.99 ± 3.00	0.864
TDCA	26.71 ± 1.71	27.99 ± 2.10	0.911
TUDCA	13.36 ± 0.86	13.99 ± 1.05	0.911

Note Continuous data are reported as the mean ± standard deviation. The Mann–Whitney U test was used to analyze continuous data. NOR = normal ovarian reserve; DOR = diminished ovarian reserve. * $P<0.05$

Correlations between bile acid metabolites and clinical characteristics

Spearman correlation analysis was used to study the relationship between BA metabolite concentrations in FF and general patient characteristics and clinical pregnancy outcomes. The results revealed that LCA, CDCA, UDCA, DCA, and CA levels were negatively correlated with baseline FSH concentration (R=-0.460, -0.348, -0.231, -0.227, -0.324) and positively correlated with baseline AMH concentration (R=0.702, 0.452, 0.408, 0.290, 0.242), AFC (R=0.616, 0.402, 0.322, 0.246, 0.213), and the number of oocytes retrieved (R=0.654, 0.432, 0.334, 0.333, 0.338). With the exception of DCA, the other four BAs (LCA, CDCA, UDCA, and CA) increased with increasing E_2 levels on the day of hCG injection (R=0.511, 0.342, 0.311, 0.231). No significant correlation was found between other BA metabolites and clinical indicators (Fig. 1F).

Establishment of a diagnostic model based on five bile acids

To facilitate earlier diagnosis and timely intervention for DOR, we constructed a random forest diagnostic model using the five BAs described above. LCA, CDCA, UDCA, DCA, and CA had significant differences in FF between the two groups and were closely associated with indicators of ovarian reserve assessment. As shown in Fig. 1G, a ROC curve was generated to evaluate the diagnostic performance of the model, which had an AUC value of 0.964. Figure 1H and I showed the mean decrease accuracy and mean decrease in the Gini coefficient of the five variables, and LCA was found to serve as the most important variables in the random forest model. When only LCA was included in the diagnostic model, the AUC value was 0.944. When the first three important variables in the model, LCA, CDCA, and UDCA, were selected, the AUC value (0.944) was comparable to that of the model only containing LCA. The model that included the five differential BAs had the highest AUC, so we ultimately chose the five-variable model for clinical efficiency. In addition, LCA is most likely to be a predictive and intervention marker for DOR.

Identifying changes in granulosa cells

To explore the possible effects of BA level changes in FF on ovarian function, we analyzed the transcriptome differences of GCs in 7 groups of patients with DOR and NOR. These 7 groups of patients were recruited from an additional cohort with the same criteria for inclusion as before. We totally identified 1136 DEGs including 482 up-regulated and 654 down-regulated genes in the DOR group compared to the NOR group (Supplemental Table 1, available online). The volcano plot illustrates the distribution of all the screened genes (Supplemental Fig. 1, available online). The top 5 up-regulated DEGs, *SYT4*, *ANKRD30BL*, *CABP1*, *NPFFR2* and *HLA-G*, exhibited over fivefold increases (e.g., *SYT4* exhibited a 8.116-fold increase). The top 5 down-regulated DEGs, *MUC5AC*, *ABCC12*, *AC239804.1*, *LINC02576* and *AC073575.2*, ranged from 7.368- to 8.315-fold decreases. It is worth noting that only 148 up-regulated DEGs met |FC| > 1, while 403 down-regulated DEGs met that, suggesting that DOR-associated dysregulation of GC's genes is mainly mediated through decreased rather than increased expression.

According to the GO biological process (BP) analysis, the primary pathways enriched in the up-regulated DEGs were the metabolic and biosynthetic processes of fatty acids, alcohols, steroids, sterols, and cholesterol (Fig. 2A). The main pathway enriched in the down-regulated DEGs was the regulation of cell–cell adhesion (Fig. 2B). KEGG functional annotation indicated that the pathways enriched in the up-regulated genes were those involving the fatty acid terpenoid backbone and ovarian steroidogenesis, while the predominant pathway enriched in the down-regulated genes was the Rap1 signaling pathway (Fig. 2C and D).

Discussion

Main findings

The aim of this study was to elucidate the changes in BA metabolites in the FF of DOR patients and to identify novel markers that could aid in the early detection of and intervention in DOR.

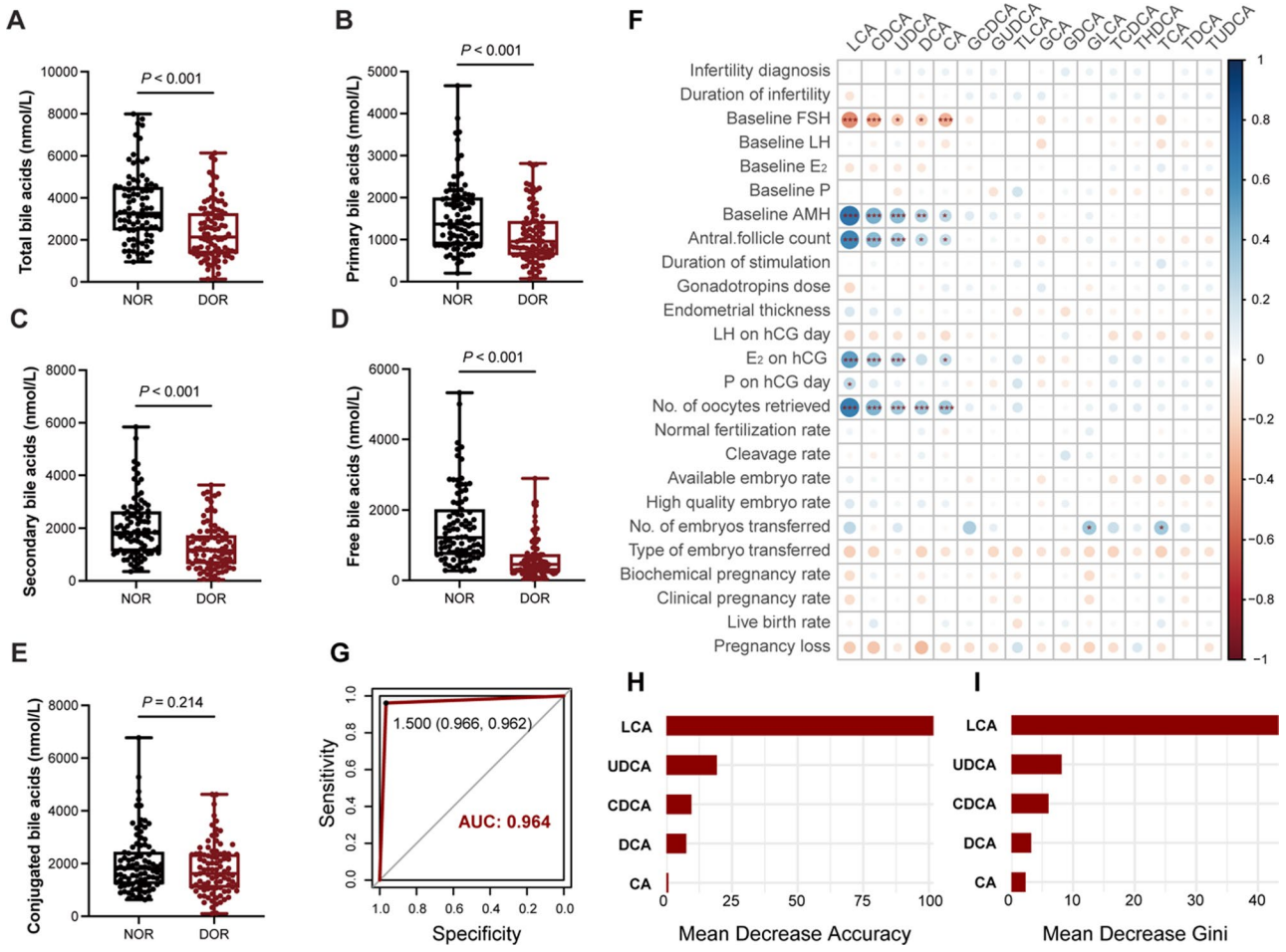

Fig. 1 Series analysis of bile acid levels in follicular fluid of patients with DOR. Follicular fluid in patients with DOR showed unique bile acid metabolism characteristics. We compared the difference of total bile acids (**A**), primary bile acids (**B**), secondary bile acids (**C**), free bile acids (**D**) and conjugated bile acids (**E**) between NOR and DOR. **(F)** The correlation between bile acid metabolite levels in follicular fluid and clinical characteristics in 182 patients (NOR = 91, DOR = 91), where the size of the dots represents the size of Spearman's correlation coefficient and significance is marked with *. We constructed a random forest diagnostic model using five bile acids, and plotted the model's ROC curve and AUC value (**G**), the mean decrease accuracy and mean decrease in the Gini coefficient of each variable (**H**,**I**). NOR = normal ovarian reserve; DOR = diminished ovarian reserve; ROC = receiver operating curve; AUC = area under the curve. * $P < 0.05$; ** $P < 0.01$; *** $P < 0.001$

Initially, we collected data from 182 patients with DOR or NOR and compared their general characteristics and clinical pregnancy outcomes. The results indicated no difference in pregnancy outcomes between DOR patients and NOR patients. Although DOR is associated with reduced oocyte number and quality, DOR patients possess functional oocytes [7]. As long as DOR patients have embryos available for transfer, their chances of pregnancy and live birth are comparable to those of patients without DOR [19, 25, 58].

Subsequently, we analyzed the BA content in the FF of both patient groups. The FF of DOR patients exhibited unique metabolic traits. Notably, LCA, CDCA, UDCA, DCA, and CA levels were significantly decreased in the FF of DOR patients. Unfortunately, no reports are available on the serum BA profiles of DOR patients.

Interpretation

Previous research has established that the ovary lacks the ability to synthesize BAs, which enter FF via passive and active transport from blood [40]. We speculate that the changes in the BA metabolite profile in the FF of DOR patients may be attributed to differences in the absorption of BA by follicles and/or alterations in the BA pool in circulation. A study in buffalo demonstrated that healthy follicles are more likely to obtain BAs from the blood due to higher expression of the BA transporter genes *NCTP* and *ASBT* and an abundance of capillaries [51]. Moreover, the content of conjugated BAs in the atretic follicles of buffalo may increase through a specific BA screening mechanism that leads to the accumulation of conjugated BAs such as GDCA in such atretic follicles, which further accelerates closure by promoting GC apoptosis and inhibiting steroid hormone production. Therefore, it is

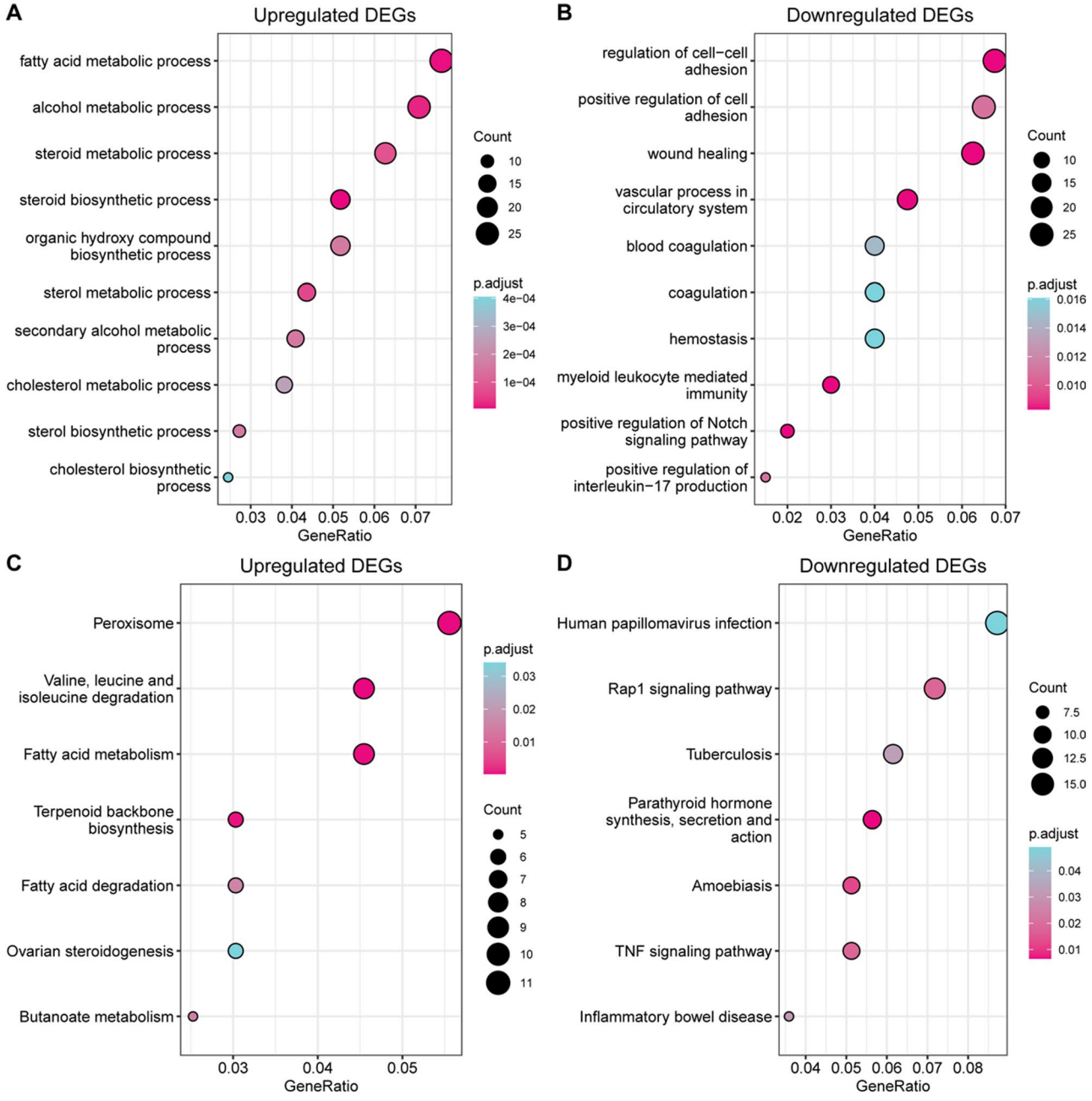

Fig. 2 GO and KEGG pathway enrichment analysis of all DEGs. (**A**) The top 10 GO BP terms enriched in the up-regulated genes. (**B**) The top 10 GO BP terms enriched in the down-regulated genes. (**C**) KEGG pathways enriched in the up-regulated genes. (**D**) KEGG pathways enriched in the down-regulated genes. GO = Gene Ontology; BP = biological process; KEGG = Kyoto Encyclopedia of Genes and Genomes

plausible that DOR leads to changes in the affinity for and absorption rate of different BA subspecies in follicles, resulting in decreases in the aforementioned five BAs and total BAs.

Another plausible explanation is that gut microbiota abnormalities in DOR patients lead to changes in the circulating BA pool, which subsequently affects the BA profile in FF. Targeted quantitative metabolomics revealed that the levels of indole-3-propionic acid (IPA) and indole-3-acetic acid (IAA) were significantly decreased in the FF of DOR patients [33]. The differences in IPA and IAA concentrations in FF may indirectly reflect changes in the generation or utilization of intestinal microbial metabolites between DOR and NOR populations, as both IPA and IAA are tryptophan-derived metabolites from intestinal flora. Also, increasing evidence suggests that gut microbiota dysbiosis is associated with POI and POF [6, 21]. One previous study clearly revealed the mechanism by which the gut microbiota–BA–interleukin-22 axis regulates the pathogenesis of PCOS [44].

Under normal conditions, conjugated CA and CDCA are first dissociated in the intestine and then combined via 7α-dehydroxylation to form DCA and LCA, respectively [23]. The 7α-hydroxyl group of CDCA undergoes isomerization to 7β to form UDCA [23]. Based on the available data, it is reasonable to infer that DOR patients have intestinal flora disorders, leading to abnormal transformation of primary BAs to secondary BAs; that is, CA and CDCA are transformed into metabolites other than DCA, LCA, and UDCA. It is necessary to further evaluate these hypotheses, such as by analyzing differential gut microflora in DOR and NOR patients and exploring whether specific flora are related to differential BA metabolites in FF.

Analysis of the correlation between the different BA metabolites and the clinical characteristics of the included patients revealed that LCA, CDCA, UDCA, DCA, and CA are closely correlated with ovarian reserve. This finding suggests that these metabolites may be potential biomarkers of DOR. In light of this, we constructed a random forest model for DOR diagnosis based on the aforementioned five BAs. This model demonstrated extremely high diagnostic value. Currently recognized indicators for evaluating ovarian reserve cannot detect DOR early, and thus intervention cannot be initiated in a timely manner. We hope to identify a more sensitive biomarker and advance the intervention window. The mean decrease accuracy and mean decrease in the Gini coefficient indicated that LCA is the most promising biomarker. In the future, we will further explore the metabolic characteristics of circulating LCA in patients with DOR with the goal of using this metabolite as a new and more sensitive independent indicator of ovarian reserve. We will also investigate the effect of LCA-targeted intervention on ovarian function, seeking new intervention and treatment strategies for DOR.

In the early stages of ovarian function decline, FSH levels gradually increase, leading to increased interactions of FSH with its receptors and subsequently increased E_2 levels. With advancing age and further decline in ovarian function, a state of high FSH and low E_2 is observed [49]. The compensatory increase in E_2 in the DOR patients included in this study indicates that they were in the early stages of ovarian function decline. Our results showed that BAs, particularly LCA, decreased in the early stages of DOR development. Changes in LCA levels occur earlier, are more dramatic than those in FSH and E_2, and are more accurate due to the lack of cyclical variability, making LCA levels more valuable for predicting and diagnosing DOR. Furthermore, LCA can serve as a marker for the extremely early prediction of DOR.

Related studies suggest that LCA is an effective anti-aging natural compound [2, 3, 15, 39]. Exogenous LCA would be dispersed into the mitochondrial inner membrane after being added to yeast cells, which would lead to the synthesis of glycerophospholipids and the remodeling of mitochondrial membrane movement, and change the size, number and morphology of mitochondria. On this basis, changes in mitochondrial respiration, membrane potential, ATP synthesis, etc., and LCA can prolong the life of yeast and slow down its aging. Moreover, LCA treatment can inhibit the production of TNF-α, a key inflammatory cytokine [55]. LCA can suppress inflammation and oxidative stress by inhibiting NLRP3 and Nrf2 signaling [45, 54]. CDCA treatment improved fasting blood glucose and mean blood glucose levels in PCOS model mice [53]. CDCA also modulates renal lipid metabolism, decreases proteinuria, and decreases renal fibrosis, inflammation, and oxidative stress [20]. UDCA therapy improved ovarian morphology and decreased total testosterone and insulin levels in a PCOS rat model [14]. UDCA has also been shown to have protective effects against oxidative stress and inflammation in various diseases [5, 24, 26, 27]. A study by Yahong Zheng et al. showed that DCA and LCA decrease NF-κB inflammatory signaling through TGR5, thus protecting the liver and inhibiting inflammation [59]. Moreover, CA can maintain blood–brain barrier integrity, decrease apoptosis, and mitigate oxidative stress and inflammatory damage after oxygen-glucose deprivation and reoxygenation [31]. As mentioned above, the antioxidative stress and anti-inflammatory properties of these five BAs have been confirmed in numerous experiments. The concentration of inflammatory factors in FF affects oocyte maturation, follicular wall rupture, fertilization, and early embryo development [34, 36]. Huang Y et al. confirmed that FF in DOR patients contains higher levels of indicators of oxidative stress and inflammation [22]. Therefore, we speculate that these five BAs are absorbed by the intestinal epithelium and enter systemic circulation, where they reach the ovary and exert anti-inflammatory and antioxidative stress effects. Given that reproductive aging is an important phenotype of DOR, LCA is most likely to be a potential intervention for DOR. However, the impact of BA metabolites on ovarian function in the context of DOR must be validated in further preclinical and clinical experiments.

Considering the pivotal role of GCs in folliculogenesis and oocyte development, examining the gene expression profile of GCs from DOR patients may offer insights into the molecular mechanisms of DOR. In our study, we found that the steroid biosynthetic process was the primary pathway enriched in the upregulated DEGs. Consistent with this finding, our DOR patients exhibited significantly higher baseline E_2 levels. We speculate that negative feedback from the low-BA ovarian environment stimulates GCs, leading to increased steroid synthesis, but GCs do not express the key genes for BA synthesis.

Ruifen He et al. reported that genes related to steroid synthesis were significantly downregulated in GCs from DOR patients [17]. Another study did not report significant differences in steroid synthesis [34]. Therefore, studies involving larger samples are needed.

Oxidative stress is closely linked with inflammation. In response to environmental stress, reactive oxygen species-induced mitochondrial DNA damage triggers the imbalanced activation of the NLRP3/NLRP6 inflammasome via the stimulation of caspase-8 and BRCC36. Activated NLRP3 in the context of suppressed NLRP6 stimulates caspase-1 activation, leading to IL-1β and IL-18 maturation and secretion [8]. Because of its inflammasome-independent function, NLRP6 has an anti-inflammatory role in the regulation of NETosis in pneumonia, gastric cancer, liver disease, rheumatoid arthritis, certain acute kidney injuries, and intestinal colitis [1]. In the dextran sulfate sodium-induced colitis model, the NLRP6 inflammasome protects against colitis by driving the release of IL-18, which promotes epithelial barrier integrity by increasing Lgr5+stem cells and antimicrobial responses. NLRP6 can also prevent colon cancer by inducing IL-18, which results in reduced intestinal inflammation and proliferation signals [10]. In our study, NLRP6 and IL-18 expression was significantly decreased in the GCs of DOR patients. IL-18 levels in FF were lower in the DOR group than in the NOR group, as confirmed by other studies [22]. Tsuji et al. demonstrated that IL-18 receptor blockade by an IL-18R monoclonal antibody reduced the number of ovulated oocytes and inhibited the expansion of cumulus cells surrounding the ovum [50]. IL-18 can directly affect the function of bovine theca cells, including the promotion of cell proliferation and steroidogenesis [57]. Therefore, based on the above results, it is reasonable to speculate that inflammatory levels increase in DOR patients via downregulation of the NLRP6–IL-18 pathway, which affects thecal cell function and follicular development, leading to follicular development disorders.

Strengths and limitations

Nevertheless, there are several limitations of our study. First, all patients included in this study received ART, including ovulation induction and other drugs, which may affect the local ovarian microenvironment and make it distinct from the natural ovarian microenvironment, potentially impacting the universality of our results. Second, the serum levels of the aforementioned metabolites should be analyzed to further clarify the levels of BAs in systemic circulation in DOR and NOR patients. Due to the lack of information on the type and content of BA in the serum of patients, the correlation between serum and follicular fluid BA is still unclear. Therefore, abnormal bile acid in follicular fluid of DOR patients may not be completely caused by abnormal bile acid metabolism in granulosa cells, which is also a limitation of this study. In the future, we will explore such related issues in depth. Third, after identifying the differentially abundant metabolites, we did not conduct cell- or animal-based experiments for validation or further study. Finally, the RNA sequencing results were based on a limited number of patients. In the future, we should conduct research with a larger sample size and use RT−PCR to further verify our findings.

To our knowledge, this is the first study to evaluate differences in BA metabolites in the FF of DOR patients. We established a diagnostic model based on metabolites and compared the gene expression profiles in GCs from patients with DOR or NOR. Steroidogenesis and inflammation play key roles in the occurrence and development of DOR. These findings suggest that BA metabolites may exert antioxidant and anti-inflammatory effects in FF, indirectly reflecting the interaction between the intestinal flora and the follicular microenvironment. In the future, it may be possible to evaluate the improvement of BA supplementation on ovarian function, which has high clinical significance.

Supplementary Information

The online version contains supplementary material available at https://doi.org/10.1186/s13048-024-01573-3.

Supplementary Material 1: The volcano plot of all the differentially expressed genes. DOWN = down-regulated; NS = no significance; UP = up-regulated; FC = fold change.

Supplementary Material 2

Acknowledgements

We would like to thank the clinical embryologists, nurses, medical doctors and other staff of Peking University Third Hospital for their support.

Author contributions

X.Q. conceived the study and managed the project throughout. S.D., W.L., X.X., S.Y., C.Y., Y.W., L.H. and M.S. were responsible for collecting and testing all clinical samples. S.D. contributed to the computational analysis of all the data and the interpretation of the results. The manuscript was written collaboratively by S.D. and W.L., X.Q., X.Z. and S.D. critically revised the manuscript and checked all data and analyses. X.Q. and J.Q. provided financial and human support for the smooth progress of the whole project. All authors critically reviewed and approved the final version of the manuscript.

Funding statement

This study was supported by the Beijing Natural Science Foundation (7242162), the National Natural Science Foundation of the Peoples' Republic of China (82288102), the China Association for Science and Technology Youth Support Talent Project (YESS20210069), and the Key Clinical Projects of Peking University Third Hospital (No. BYSY2022045).

Data availability

No datasets were generated or analysed during the current study.

Declarations

Ethical approval

This study was approved by the Ethics Committee of Medical Scientific Research at Peking University Third Hospital, and informed consent was obtained from all participants (Peking University Third Hospital Ethics Committee No. M2023152; Approval date: 2023.03.14).

Competing interests

The authors declare no competing interests.

Author details

[1]State Key Laboratory of Female Fertility Promotion, Center for Reproductive Medicine, Department of Obstetrics and Gynecology, Peking University Third Hospital, Beijing, China
[2]Peking University People's Hospital, Beijing, P. R. China
[3]National Clinical Research Center for Obstetrics and Gynecology, Peking University Third Hospital, Beijing, China
[4]Key Laboratory of Assisted Reproduction (Peking University), Ministry of Education, Beijing, China
[5]Beijing Key Laboratory of Reproductive Endocrinology and Assisted Reproductive Technology, Beijing, China
[6]Peking University Third Hospital, Beijing, China

Received: 23 October 2024 / Accepted: 4 December 2024
Published online: 19 December 2024

References

1 Angosto-Bazarra D, Molina-López C, Pelegrín P. Physiological and pathophysiological functions of NLRP6: pro- and anti-inflammatory roles. Commun Biol. 2022;5(1):524.
2 Beach A, Richard VR, Bourque S, Boukh-Viner T, Kyryakov P, Gomez-Perez A, et al. Lithocholic bile acid accumulated in yeast mitochondria orchestrates a development of an anti-aging cellular pattern by causing age-related changes in cellular proteome. Cell Cycle. 2015;14(11):1643–56.
3 Beach A, Richard VR, Leonov A, Burstein MT, Bourque SD, Koupaki O, et al. Mitochondrial membrane lipidome defines yeast longevity. Aging. 2013;5(7):551–74.
4 Bunnewell SJ, Honess ER, Karia AM, Keay SD, Al Wattar BH, Quenby S. Diminished ovarian reserve in recurrent pregnancy loss: a systematic review and meta-analysis. Fertil Steril. 2020;113(4):818–e8273.
5 Cao A, Wang L, Chen X, Guo H, Chu S, Zhang X, et al. Ursodeoxycholic acid ameliorated Diabetic Nephropathy by attenuating hyperglycemia-mediated oxidative stress. Biol Pharm Bull. 2016;39(8):1300–8.
6 Cao LB, Leung CK, Law PW, Lv Y, Ng CH, Liu HB, et al. Systemic changes in a mouse model of VCD-induced premature ovarian failure. Life Sci. 2020;262:118543.
7 Cedars MI. Evaluation of female Fertility-AMH and Ovarian Reserve Testing. J Clin Endocrinol Metab. 2022;107(6):1510–9.
8 Chi W, Hua X, Chen X, Bian F, Yuan X, Zhang L, et al. Mitochondrial DNA oxidation induces imbalanced activity of NLRP3/NLRP6 inflammasomes by activation of caspase-8 and BRCC36 in dry eye. J Autoimmun. 2017;80:65–76.
9 Chiang JYL, Ferrell JM. Bile acids as metabolic regulators and nutrient sensors. Annu Rev Nutr. 2019;39:175–200.
10 Chou WC, Jha S, Linhoff MW, Ting JP. The NLR gene family: from discovery to present day. Nat Rev Immunol. 2023;23(10):635–54.
11 de la Barca JMC, Boueilh T, Simard G, Boucret L, Ferré-L'Hotellier V, Tessier L, et al. Targeted metabolomics reveals reduced levels of polyunsaturated choline plasmalogens and a smaller dimethylarginine/arginine ratio in the follicular fluid of patients with a diminished ovarian reserve. Hum Reprod. 2017;32(11):2269–78.
12 Dumesic DA, Meldrum DR, Katz-Jaffe MG, Krisher RL, Schoolcraft WB. Oocyte environment: follicular fluid and cumulus cells are critical for oocyte health. Fertil Steril. 2015;103(2):303–16.
13 Farquhar CM, Bhattacharya S, Repping S, Mastenbroek S, Kamath MS, Marjoribanks J, et al. Female subfertility. Nat Rev Dis Primers. 2019;5(1):7.
14 Gozukara I, Dokuyucu R, Özgür T, Özcan O, Pınar N, Kurt RK, et al. Histopathologic and metabolic effect of ursodeoxycholic acid treatment on PCOS rat model. Gynecol Endocrinol. 2016;32(6):492–7.
15 Han B, Lv X, Liu G, Li S, Fan J, Chen L, et al. Gut microbiota-related bile acid metabolism-FXR/TGR5 axis impacts the response to anti-α4β7-integrin therapy in humanized mice with colitis. Gut Microbes. 2023;15(1):2232143.
16 Han S, Zhai Y, Guo Q, Qin Y, Liu P. Maternal and neonatal complications in patients with diminished Ovarian Reserve in In-Vitro Fertilization/Intracytoplasmic sperm injection cycles. Front Endocrinol (Lausanne). 2021;12:648287.
17 He R, Zhao Z, Yang Y, Liang X. Using bioinformatics and metabolomics to identify altered granulosa cells in patients with diminished ovarian reserve. PeerJ. 2020;8:e9812.
18 Hosseinzadeh P, Wild RA, Hansen KR. Diminished ovarian reserve: risk for preeclampsia in in vitro fertilization pregnancies. Fertil Steril. 2023;119(5):802–3.
19 Hu S, Xu B, Jin L. Perinatal outcome in young patients with diminished ovarian reserve undergoing assisted reproductive technology. Fertil Steril. 2020;114(1):118–e1241.
20 Hu Z, Ren L, Wang C, Liu B, Song G. Effect of chenodeoxycholic acid on fibrosis, inflammation and oxidative stress in kidney in high-fructose-fed Wistar rats. Kidney Blood Press Res. 2012;36(1):85–97.
21 Huang F, Cao Y, Liang J, Tang R, Wu S, Zhang P, et al. The influence of the gut microbiome on ovarian aging. Gut Microbes. 2024;16(1):2295394.
22 Huang Y, Cheng Y, Zhang M, Xia Y, Chen X, Xian Y, et al. Oxidative stress and inflammatory markers in ovarian follicular fluid of women with diminished ovarian reserve during in vitro fertilization. J Ovarian Res. 2023;16(1):206.
23 Jia W, Xie G, Jia W. Bile acid-microbiota crosstalk in gastrointestinal inflammation and carcinogenesis. Nat Rev Gastroenterol Hepatol. 2018;15(2):111–28.
24 Jiang C, Shen D, Li K, Wang H, Sang W, Qi H. Protective effects of Ursodeoxycholic Acid against oxidative stress and Neuroinflammation through Mitogen-activated protein kinases pathway in MPTP-Induced Parkinson Disease. Clin Neuropharmacol. 2022;45(6):168–74.
25 Kawwass JF, Hipp HS, Session DR, Kissin DM, Jamieson DJ, National ART, Surveillance System Group. Severity of diminished Ovarian Reserve and Chance of Success with assisted Reproductive Technology. J Reprod Med. 2017;62(3–4):153–60.
26 Koc S, Aktas A, Sahin B, Ozer H, Zararsiz GE. Protective effect of ursodeoxycholic acid and resveratrol against tacrolimus induced hepatotoxicity. Biotech Histochem. 2023;98(7):471–8.
27 Lakić B, Škrbić R, Uletilović S, Mandić-Kovačević N, Grabež M, Šarić MP et al. Beneficial Effects of Ursodeoxycholic Acid on Metabolic Parameters and Oxidative Stress in Patients with Type 2 Diabetes Mellitus: A Randomized Double-Blind, Placebo-Controlled Clinical Study. *J Diabetes Res* 2024; 2024:4187796.
28 Lavelle A, Sokol H. Gut microbiota-derived metabolites as key actors in inflammatory bowel disease. Nat Rev Gastroenterol Hepatol. 2020;17(4):223–37.
29 Li A, Li F, Song W, Lei ZL, Sha QQ, Liu SY, et al. Gut microbiota-bile acid-vitamin D axis plays an important role in determining oocyte quality and embryonic development. Clin Transl Med. 2023;13(10):e1236.
30 Li A, Li F, Song W, Lei ZL, Zhou CY, Zhang X, et al. Maternal exposure to 4-vinylcyclohexene diepoxide during pregnancy leads to disorder of gut microbiota and bile acid metabolism in offspring. Ecotoxicol Environ Saf. 2024;269:115811.
31 Li C, Wang X, Yan J, Cheng F, Ma X, Chen C et al. Cholic Acid Protects In Vitro Neurovascular Units against Oxygen and Glucose Deprivation-Induced Injury through the BDNF-TrkB Signaling Pathway. *Oxid Med Cell Longev* 2020; 2020:1201624.
32 Li J, Zhang Z, Wei Y, Zhu P, Yin T, Wan Q. Metabonomic analysis of follicular fluid in patients with diminished ovarian reserve. Front Endocrinol (Lausanne). 2023;14:1132621.
33 Liu A, Shen H, Li Q, He J, Wang B, Du W, et al. Determination of tryptophan and its indole metabolites in follicular fluid of women with diminished ovarian reserve. Sci Rep. 2023;13(1):17124.
34 Liu L, Cai B, Zhang X, Tan J, Huang J, Zhou C. Differential transcriptional profiles of human cumulus granulosa cells in patients with diminished ovarian reserve. Arch Gynecol Obstet. 2022;305(6):1605–14.
35 Liu Y, Li Z, Wang Y, Cai Q, Liu H, Xu C, et al. IL-15 participates in the pathogenesis of polycystic ovary syndrome by affecting the activity of Granulosa cells. Front Endocrinol (Lausanne). 2022;13:787876.
36 Liu Y, Liu H, Li Z, Fan H, Yan X, Liu X, et al. The release of Peripheral Immune Inflammatory cytokines promote an inflammatory Cascade in PCOS patients via altering the Follicular Microenvironment. Front Immunol. 2021;12:685724.
37 Lu Q, Shen H, Li Y, Zhang C, Wang C, Chen X, et al. Low testosterone levels in women with diminished ovarian reserve impair embryo implantation rate: a retrospective case-control study. J Assist Reprod Genet. 2014;31(4):485–91.

38 Lu YJ, Li Q, Chen LX, Tian T, Kang J, Hao YX, et al. Association between maternal MTHFR C677T/A1298C combination polymorphisms and IVF/ICSI outcomes: a retrospective cohort study. Hum Reprod Open. 2022;2023(1):hoac055.
39 Luu TH, Bard JM, Carbonnelle D, Chaillou C, Huvelin JM, Bobin-Dubigeon C, et al. Lithocholic bile acid inhibits lipogenesis and induces apoptosis in breast cancer cells. Cell Oncol (Dordr). 2018;41(1):13–24.
40 Nagy RA, Hollema H, Andrei D, Jurdzinski A, Kuipers F, Hoek A, et al. The origin of follicular bile acids in the human ovary. Am J Pathol. 2019;189(10):2036–45.
41 Nagy RA, van Montfoort AP, Dikkers A, van Echten-Arends J, Homminga I, Land JA, et al. Presence of bile acids in human follicular fluid and their relation with embryo development in modified natural cycle IVF. Hum Reprod. 2015;30(5):1102–9.
42 Pastore LM, Christianson MS, Stelling J, Kearns WG, Segars JH. Reproductive ovarian testing and the alphabet soup of diagnoses: DOR, POI, POF, POR, and FOR. J Assist Reprod Genet. 2018;35(1):17–23.
43 Pecker LH, Hussain S, Mahesh J, Varadhan R, Christianson MS, Lanzkron S. Diminished ovarian reserve in young women with sickle cell anemia. Blood. 2022;139(7):1111–5.
44 Qi X, Yun C, Sun L, Xia J, Wu Q, Wang Y, et al. Gut microbiota-bile acid-interleukin-22 axis orchestrates polycystic ovary syndrome. Nat Med. 2019;25(8):1225–33.
45 Shao J, Ge T, Tang C, Wang G, Pang L, Chen Z. Synergistic anti-inflammatory effect of gut microbiota and lithocholic acid on liver fibrosis. Inflamm Res. 2022;71(10–11):1389–401.
46 Shen H, Wang L, Gao M, Wei L, Liu A, Wang B, et al. The follicular fluid metabolome in infertile individuals between polycystic ovary syndrome and diminished ovarian reserve. Arch Biochem Biophys. 2022;732:109453.
47 Shirasuna K, Iwata H. Effect of aging on the female reproductive function. Contracept Reprod Med. 2017;2:23.
48 Singh J, Metrani R, Shivanagoudra SR, Jayaprakasha GK, Patil BS. Review on bile acids: effects of the gut microbiome, interactions with Dietary Fiber, and alterations in the bioaccessibility of Bioactive compounds. J Agric Food Chem. 2019;67(33):9124–38.
49 Tal R, Seifer DB. Ovarian reserve testing: a user's guide. Am J Obstet Gynecol. 2017;217(2):129–40.
50 Tsuji Y, Tamaoki TH, Hasegawa A, Kashiwamura S, Iemoto A, Ueda H, et al. Expression of interleukin-18 and its receptor in mouse ovary. Am J Reprod Immunol. 2001;46(5):349–57.
51 Wei Y, Cheng J, Luo M, Yang S, Xing Q, Cheng J, et al. Targeted metabolomics analysis of bile acids and cell biology studies reveal the critical role of glycodeoxycholic acid in buffalo follicular atresia. J Steroid Biochem Mol Biol. 2022;221:106115.
52 Wu Q, Liang X, Wang K, Lin J, Wang X, Wang P, et al. Intestinal hypoxia-inducible factor 2α regulates lactate levels to shape the gut microbiome and alter thermogenesis. Cell Metab. 2021;33(10):1988–e20037.
53 Yang YL, Zhou WW, Wu S, Tang WL, Wang ZW, Zhou ZY, et al. Intestinal Flora is a key factor in insulin resistance and contributes to the development of polycystic ovary syndrome. Endocrinology. 2021;162(10):bqab118.
54 Yao B, He J, Yin X, Shi Y, Wan J, Tian Z. The protective effect of lithocholic acid on the intestinal epithelial barrier is mediated by the vitamin D receptor via a SIRT1/Nrf2 and NF-κB dependent mechanism in Caco-2 cells. Toxicol Lett. 2019;316:109–18.
55 Yoneno K, Hisamatsu T, Shimamura K, Kamada N, Ichikawa R, Kitazume MT, et al. TGR5 signalling inhibits the production of pro-inflammatory cytokines by in vitro differentiated inflammatory and intestinal macrophages in Crohn's disease. Immunology. 2013;139(1):19–29.
56 Zegers-Hochschild F, Adamson GD, Dyer S, Racowsky C, de Mouzon J, Sokol R, Rienzi L, et al. The International Glossary on Infertility and Fertility Care, 2017. Fertil Steril. 2017;108(3):393–406.
57 Zhang HY, Zhu FF, Zhu YJ, Hu YJ, Chen X. Effects of IL-18 on the proliferation and steroidogenesis of bovine theca cells: possible roles in the pathogenesis of polycystic ovary syndrome. J Cell Mol Med. 2021;25(2):1128–39.
58 Zhao M, Huan Q, Huang L, Yang L, Dong M. Pregnancy outcomes of intrauterine insemination in young patients with diminished ovarian reserve: a multicenter cohort study. Eur J Med Res. 2023;28(1):402.
59 Zheng X, Chen T, Jiang R, Zhao A, Wu Q, Kuang J. Hyocholic acid species improve glucose homeostasis through a distinct TGR5 and FXR signaling mechanism. Cell Metab. 2021;33(4):791–e8037.
60 Zheng Y, Yue C, Zhang H, Chen H, Liu Y, Li J. Deoxycholic acid and Lithocholic Acid Alleviate Liver Injury and inflammation in mice with Klebsiella pneumoniae-Induced Liver Abscess and Bacteremia. J Inflamm Res. 2021;14:777–89.

Publisher's note